OPTIMIZED NUMERICAL ANNULAR FLOW DRYOUT MODEL USING THE DRIFT-FLUX MODEL IN TUBE GEOMETRY

JI-HAN CHUN[1] and UN-CHUL LEE[*]
[1]BK21 Research Division of Seoul National University for Energy Resource
[*]Department of Nuclear Engineering, Seoul National University,
599 Gwanangno, Gwanak-gu, Seoul 151-742, Korea
[*]Corresponding author. E-mail : uclee@snu.ac.kr

Received January 17, 2008
Accepted for Publication April 16, 2008

Many experimental analyses for annular film dryouts, which is one of the Critical Heat Flux (CHF) mechanisms, have been performed because of their importance. Numerical approaches must also be developed in order to assess the results from experiments and to perform pre-tests before experiments. Various thermal-hydraulic codes, such as RELAP, COBRA-TF, MARS, etc., have been used in the assessment of the results of dryout experiments and in experimental pre-tests. These thermal-hydraulic codes are general tools intended for the analysis of various phenomena that could appear in nuclear power plants, and many models applying these codes are unnecessarily complex for the focused analysis of dryout phenomena alone. In this study, a numerical model was developed for annular film dryout using the drift-flux model from uniform heated tube geometry. Several candidates of models that strongly affect dryout, such as the entrainment model, deposition model, and the criterion for the dryout point model, were tested as candidates for inclusion in an optimized annular film dryout model. The optimized model was developed by adopting the best combination of these candidate models, as determined through comparison with experimental data. This optimized model showed reasonable results, which were better than those of MARS code.

KEYWORDS : Dryout, Drift-Flux Model, Entrainment/Deposition, Critical Thickness Concept

1. INTRODUCTION

CHF (Critical Heat Flux) is the phenomenon that occurs when the temperature of a heated surface is suddenly increased due to a decrease in the heat transfer coefficient, which results from the phase change of fluid at the heated surface from liquid to vapor. CHF is very important in nuclear power plants because this sudden temperature increase in nuclear fuel leads to the failure of nuclear fuel, and fuel failure is the reason that radioactive materials leak into the environment. CHF is considered to be an important parameter of the heat transfer regime in thermal-hydraulic codes. Therefore, the accurate prediction of CHF is emphasized as a key point in nuclear safety. CHF is classified as involving two kinds of mechanism. The first is Departure Nucleate Boiling (DNB), which occurs when the vapor blanket is located at the heated surface. It occurs when the surface heat flux is relatively high and the void quality is low, and it has been the major safety concern of pressurized water reactor (PWR) transients. Another mechanism is that of annular film dryout, in which a continuous liquid film on the heated surface is dried out by droplet entrainment and evaporation. The dryout mechanism has been the main safety concern of not only boiling water reactor transients, but also of the PWR transients. Dryout occurs in an annular flow regime when the void quality is relatively high [1].

Most of the thermal-hydraulic transient codes for PWRs use a CHF look-up table method, or experimental CHF correlations specific to fuel design. Since DNB has been the major safety issue of PWR safety, there are a lot of experimental databases available for DNB. However, there are few experimental and analytical databases for the dryout point, because it is only very recently that dryout models have been highlighted in PWR analysis. With the introduction of the best-estimation analysis to the design-basis and to the beyond design-basis accident analysis, core and steam generator dryout phenomena have been emphasized for the realistic prediction of transient system response.

For these reasons, much experimental research has been performed during the last few decades. To assess these experiments, numerical approaches have been developed alongside the development of experimental

approaches. Up to this point, thermal-hydraulic codes such as RELAP, COBRA-TF, MARS, etc., have been used for those tasks. Because almost all thermal-hydraulic codes have been developed for the analysis of a variety of phenomena which could exist in nuclear power plants, there are continuity equations, momentum equations, and energy equations for each phase, and many of these equations are in the codes. However, these very complex equations are unnecessary for the calculation of the dryout critical heat flux alone.

To avoid the complexities of general thermal-hydraulic codes for the calculation of dryout alone, a numerical annular flow dryout model was developed using simplified, rather than full, equations for each phase in this study. It was important for the development of the numerical annular flow dryout model that a combination of models be incorporated to calculate the velocity, fraction, and mass flux of each phase. The drift-flux model was used for the calculation of the velocity and fraction of each phase in this study. After several models of entrainment, deposition, and dryout point criterion were selected, a combination of some of these candidates was developed as a model. The optimized model using the best combination out of these candidates, chosen through comparison with experimental CHF data, and incorporating a drift-flux model, was developed. It is expected that development of an accurate and optimized numerical model for annular film dryout will be useful for the assessment of experimental data, as well as to perform pre-tests before experiments.

2. ANNULAR FLOW DRYOUT MODEL USING A DRIFT-FLUX MODEL IN TUBE GEOMETRY

There are some flow regimes from sub-cooled liquid, to annular flow in a tube. These are sub-cooled liquid, bubbly flow, slug flow, and annular flow. The sub-cooled liquid has a single phase, liquid, while the bubbly and slug flows each have two phases, as liquid and vapor, and the annular flow has three phases, as liquid film, vapor, and liquid droplets. The important thing in the development of a dryout model is the calculation methodology of the velocity and fraction of each phase. To determine these parameters, the drift-flux model was used in this study.

2.1 Sub-Cooled Liquid Flow Regime

The calculation in this flow regime is relatively simple. The energy balance equation is used to calculate the saturation point as follows:

$$q''\pi D = G\frac{1}{4}\pi D^2 C_{pl}\frac{T_{sat}-T_{l,in}}{z_{sat}}$$

$$z_{sat} = \frac{(T_{sat}-T_{f,in})GC_{pl}D}{4q''} \tag{1}$$

2.2 Bubbly and Slug flow regime

After the liquid reaches its saturation point, bubbles are generated. The frequency of bubble generation is not only increased, but these bubbles also coalesce to form slug flow along the length. These two regimes have various bubble sizes. However, except for the difference in the relative behaviors of the vapor and liquid due to the different bubble size, the general mechanism of two-phase flow can be applied equally. The following equations, which are generally used in the analysis of two-phase flow, can be used both in bubbly and slug regimes:

$$u_g = V_{gj} + j \tag{2}$$

$$G = \rho_g u_g \alpha_g + \rho_f u_f (1-\alpha_g) \tag{3}$$

Equation (2) is from the definition of drift velocity, and j is the volumetric flux, defined as the total volumetric flow rate over the flow area. Equation (3) is from mass conservation.

$$u_g = \frac{G_g}{\rho_g \alpha_g} = \frac{Gx}{\rho_g \alpha_g}, \text{ and } u_f = \frac{G_f}{\rho_f \alpha_f} = \frac{G(1-x)}{\rho_f (1-\alpha_g)}$$

Equation (4) is obtained from the ratio of the above equations, as follows:

$$\frac{u_g}{u_f} = \frac{x}{1-x}\frac{\rho_f}{\rho_g}\frac{1-\alpha_g}{\alpha_g} \tag{4}$$

Here, x is local quality, expressed as follows in the saturation:

$$x = \frac{4q''}{DGh_{fg}}(z - z_{sat})$$

As mentioned above, the relative motions are different in bubbly and slug regimes due to bubble size. The relative motion can be represented by the drift velocity of the drift-flux model. The following drift velocity equations, suggested by Zuber in [2], were adopted:

$$V_{gj} = \begin{cases} 1.41\left[\dfrac{\sigma g(\rho_f - \rho_g)}{\rho_f^2}\right]^{1/4} & \alpha_g < 0.3 \\ 0.345\left[\dfrac{gD(\rho_f - \rho_g)}{\rho_f}\right]^{1/2} & \alpha_g \geq 0.3 \end{cases} \tag{5}$$

Using the above equations, the three unknowns of u_g, u_f, and α_g can be obtained using the iteration method. Iteration is performed as shown in Fig. 1.

After this, mass flow fluxes for each phase, G_g and G_f, are obtained as:

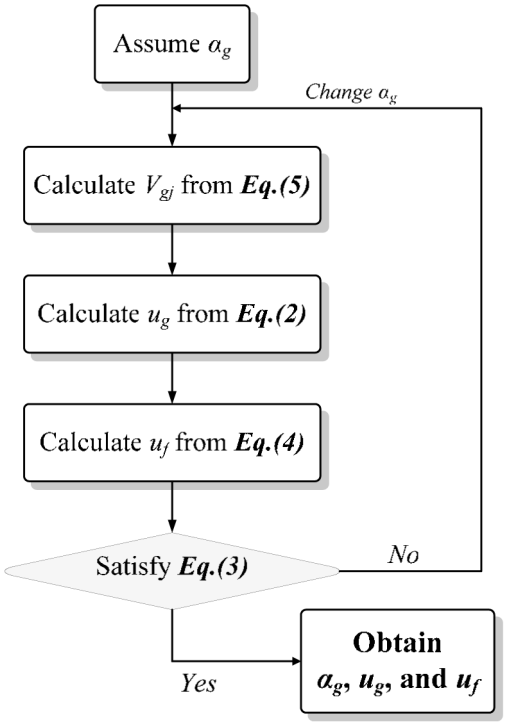

Fig. 1. Flow Chart of the Calculation for Bubbly and Slug Flow Regimes

$$G_g = \alpha_g \rho_g u_g, \quad G_f = \alpha_f \rho_f u_f \tag{6}$$

Where, the liquid fraction α_f is (1- α_g).

2.3 Annular Flow Regime

The setting of the criterion of transition to annular flow is also important in the development of a dryout model.. The annular flow transition criterion was substituted with that used in RELAP5, which has been proven through its use in various situations [3].

$$\alpha_{SA} = max\ \left[0.7\ ,\ min\ \left(\alpha^f_{crit}\ ,\ \alpha^e_{crit}\ ,\ 0.8\right)\right] \tag{7}$$

Where, $\alpha^f_{crit} = \frac{1}{v_g}\left[\frac{gD\left(\rho_f - \rho_g\right)}{\rho_g}\right]^{1/2}$ and $\alpha^e_{crit} = \frac{3.2}{v_g}\left[\frac{g\sigma\left(\rho_f - \rho_g\right)}{\rho_g^2}\right]^{1/4}$

In annular flow, the liquid phase exists as a liquid film in the tube, vapor flows through the center of the tube, and the liquid droplets enter into the vapor phase due to the velocity difference of the vapor and the liquid film. It is different from the other phases in that the three phases of vapor, liquid film, and liquid droplets occur at once. The liquid film decreases gradually along the length of the tube due to mass transfer between each phase, through mechanisms such as evaporation, entrainment, and deposition. The evaporation mass flow rate can be expressed as the following equation:

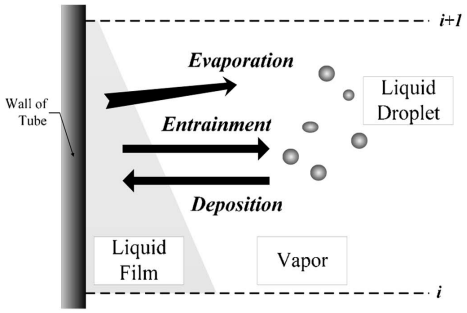

Fig. 2. Mass Transfer in Annular Flow

$$\dot{m}_{evap} = \frac{q''}{h_{fg}}\left(P_W \Delta z\right) \tag{8}$$

Entrainment is a mass transfer from the liquid film to the liquid droplet phase; because the vapor has a high velocity, some of the liquid from the liquid film forms droplets. Deposition is the process opposite that of entrainment. There are some correlations representing entrainment and deposition, and these correlations are discussed in the next chapter. The three mechanisms involved in annular flow are described in Fig. 2.

The mass fluxes at the next node were obtained using known mass transfer amounts, which could be calculated from correlations.

$$G_{g,i+1} = G_{g,i} + G_{evap} \tag{9}$$

$$G_{f,i+1} = G_{f,i} - G_{evap} - G_{ent} + G_{dep} \tag{10}$$

$$G_{e,i+1} = G_{e,i} + G_{ent} - G_{dep} \tag{11}$$

Where the subscript *i* is the node number.

After calculating mass fluxes, the velocity and fraction of the three phases should be calculated in order to obtain the liquid film thickness, which was used as the criterion to define the parameters regarding whether dryout occurred. To obtain these parameters, the definition of drift velocity was also used. Ishii semi-analytically developed the vapor drift velocity for annular flow in [4] as:

$$V_{gj}^2 = \frac{16\sqrt{\alpha}}{\rho_g f_i}\left[\frac{\mu_f j_f}{D} + \frac{\left(\rho_f - \rho_g\right)gD(1-\alpha)^3}{48}\right]$$

for laminar flow in the liquid flow

$$V_{gj}^2 = \frac{(1-\alpha)^3\sqrt{\alpha}D}{\rho_g f_i}\left[\frac{0.005\rho_f j_f |j_f|}{D(1-\alpha)^3} + \frac{(\rho_f - \rho_g)g}{3}\right]$$

for turbulent flow in the liquid flow (12)

Ishii suggested Re_f =3200 as the transition from laminar to turbulent flow during liquid flow. Using the above vapor drift velocity and the definition of this drift velocity in equation (2), we obtained the vapor velocity u_g. Because the vapor mass flux is already known, the void fraction was obtained as:

$$\alpha_g = \frac{G_g}{\rho_g u_g}$$

To calculate the liquid film velocity, the definition of volumetric flux (j) was substituted into equation (2).

$$u_f = u_g - V_{gj} \Big/ (1-\alpha_g) \quad (13)$$

Next, we can obtain the liquid film velocity, the fraction of the liquid droplet, and the liquid droplet velocity using the following equations:

$$\alpha_f = \frac{G_f}{\rho_f u_f}$$
$$\alpha_e = 1-(\alpha_g + \alpha_f)$$
$$u_e = \frac{G_e}{\rho_f \alpha_e}$$

The liquid film thickness δ results from the liquid fraction α_f.

$$\delta = \frac{D}{2}\left(1-\sqrt{1-\alpha_f}\right) \quad (14)$$

The criterion of the dryout point is crucial to the analysis of the dryout critical heat flux. We discuss this in the next section in some detail.

3. OPTIMIZED ANNULAR FLOW DRYOUT MODEL

As mentioned in the previous section, the entrainment, deposition, and the criterion of the dryout point are very important to the accuracy of dryout calculations. The optimized combination of the correlations suitable for the annular flow dryout model with the drift-flux model was found through comparing calculated dryout CHF to experimental CHF data.

3.1 Entrainment and Deposition

There are many correlations related to the entrainment and deposition phenomena of the liquid droplet phase. Although the transferred fraction due to these phenomena is small, the transferred mass is large because liquid drops have a high density, so these phenomena strongly affect the dryout. Three candidates were selected for this study.

The first candidate is the Wurtz correlation that is used in the COBRA-TF sub-channel analysis thermal-hydraulic code. The prediction ability of COBRA-TF for entrainment is well known, so the Wurtz correlation can be referred to indirectly as a proven correlation [5].

$$\dot{m}_{ent} = 2.0\frac{k_s \tau_i u_g \mu_f}{\sigma^2}(P_W \Delta z) \quad (15)$$

$$\dot{m}_{dep} = 0.01 C_D (P_W \Delta z) \quad (16)$$

Where k_s is the equivalent sand roughness determined from experimental values, τ_i is the interfacial shear stress, and C_D is the mean concentration of liquid droplets in the core.

$$k_s = 0.57\delta + 21.73\times10^3\delta^2 - 38.8\times10^6\delta^3 + 55.68\times10^9\delta^4$$
$$\tau_i = 0.005(1+75\alpha_f)\rho_g(u_g - u_f)^2$$
$$C_D = \frac{\alpha_e \rho_f}{\alpha_e + \alpha_g}$$

The second candidate is the Sugawara correlation. This correlation was developed to improve the weakness of the Wurtz correlation for low pressure and low mass flux situations, through the addition of a density ratio [6].

$$\dot{m}_{ent} = 1.07\left(\frac{\tau_i \Delta h_{eq}}{\sigma}\right)\left(\frac{u_g \mu_f}{\sigma}\right)\left(\frac{\rho_f}{\rho_g}\right)^{0.4}(P_W \Delta z) \quad (17)$$

Where,

$$\Delta h_{eq} = k_s \quad \text{for } Re_g > 1\times10^5$$
$$\Delta h_{eq} = k_s\left[2.136\log_{10}(\mathrm{Re}_g) - 9.68\right] \quad \text{for } Re_g \le 1\times10^5$$

$$\dot{m}_{dep} = 9.0\times10^{-3}\left(\frac{C_D}{\rho_g}\right)^{-0.5}\mathrm{Re}_g^{-0.2}\, Sc^{-2.3} u_g C_D (P_W \Delta z) \quad (18)$$

The third candidate was suggested by Ezzidi. This correlation was developed to modify the Suganwara correlation for its application to the COBRA-TF code. Ezzidi et.al. put the Sugawara correlation into the COBRA-TF, and found that the Sugawara correlation over-estimated the entrainment rate in the COBRA-TF, so the Sugawara correlation was improved through

multiplying it by the ratio of the Reynolds number [7].

$$\dot{m}_{ent} = 1.07\left(\frac{\tau_i \Delta h_{eq}}{\sigma}\right)\left(\frac{u_g \mu_f}{\sigma}\right)\left(\frac{\rho_f}{\rho_g}\right)^{0.4}\left(\frac{\mathrm{Re}_f}{\mathrm{Re}_{gf}}\right)^{0.4}\left(P_W \Delta z\right) \qquad (19)$$

Where,

$$\Delta h_{eq} = k_s \qquad \text{for } Re_g > 1\times10^5$$

$$\Delta h_{eq} = k_s\left[\log_{10}\left(\frac{\mathrm{Re}_g}{34028}\right)^{2.39232}\right] \qquad \text{for } Re_g \le 1\times10^5$$

$$\dot{m}_{dep} = 9.0\times10^{-3}\left(\frac{C_D}{\rho_g}\right)^{-0.5}\mathrm{Re}_g^{-0.2}\,Sc^{-2.3}\,u_g C_D\left(P_W \Delta z\right)$$

3.2 Criterion of the Dryout Point

The traditional concept of the criterion for dryout is the heat flux when the liquid mass flux or liquid film thickness is zero. However, Chun suggested in his critical thickness concept that the liquid film disappears instantly when the film is thinner than the critical thickness. This concept was assessed in order to increase the accuracy of dryout calculations and find the accurate position of dryout, especially in non-uniform heated situations. The Chun correlation is expressed in the following equation [8]:

$$\delta_{critical} = \left(\frac{q''}{h_{fg} G_{f,h}}\right)^{0.35}\frac{v_{fg}\mu_l^2}{\sigma}\times 10^{8.8\left(\frac{\mu_g}{\mu_l}\right)^{0.617}} \qquad (20)$$

Chun suggested the application range of this correlation as shown in Table 1.

In this study, two kinds of candidates were selected. The first candidate is the case without the critical thickness concept, which determines dryout when the liquid film thickness is equal to zero, as mentioned above. The second candidate is with the critical thickness concept, which determines dryout when the liquid film thickness is less than the critical thickness.

Table 1. Application Range of Critical film thickness Correlation

Parameters	Range
Pressure	0.5 - 12.0 Mpa
Mass Flux	100.0 - 2000.0 kg/m^{2}s
Local Quality	0.1 - 0.9

3.3 Optimization of the Dryout Model through a Combination of Correlations

In this study, three candidates for the entrainment and deposition models and two concepts for the criterion of the dryout point were selected. Six combinations for these various models were generated, as shown in Table 2:

To determine the optimized combination, each combination was assessed for its accuracy by comparing

Table 2. Combination of Models

Case	Applied Models
Case 1	***Wurtz*** **correlation** for entrainment/deposition Criterion of dryout ***without*** critical thickness concept
Case 2	***Wurtz*** **correlation** for entrainment/deposition Criterion of dryout ***with*** critical thickness concept
Case 3	***Sugawara*** **correlation** for entrainment/deposition Criterion of dryout ***without*** critical thickness concept
Case 4	***Sugawara*** **correlation** for entrainment/deposition Criterion of dryout ***with*** critical thickness concept
Case 5	***Ezzidi*** **correlation** for entrainment/deposition Criterion of dryout ***without*** critical thickness concept
Case 6	***Ezzidi*** **correlation** for entrainment/deposition Criterion of dryout ***with*** critical thickness concept

Table 3. Experimental Condition of Assessments

	Number of data	Diameter(mm)	Length(m)	Pressure(bar)	Mass flux(kg/m^{2}s)
KAIST Databank	88	17.5 – 25.00	1.95 – 3.75	19.61 – 68.95	231.0 – 1916.0
Becker	70	6.07 – 13.06	0.60 – 3.00	3.14 – 69.6	113.6 – 1731.3

it with several sets of critical heat flux experimental data. The Becker CHF test and the KAIST CHF databank were used. This data was examined under the various conditions of tube geometry shown in Table 3 [9,10]:

4. RESULTS AND DISCUSSIONS

Figures 3 to 8 present the results of each case, comparing CHF experimental data. These figures were expressed as relative error versus pressure and mass flux to analyze the accuracy of these parameters. The relative error is expressed as follows:

$$Relative\ \ Error = \frac{q''_{c,cal} - q''_{c,exp}}{q''_{c,exp}} \tag{21}$$

Table 4 shows the statistics of each case. The mean error, RMS (Root Mean Square) error, and standard deviation in the table were calculated using the following equations:

$$Mean\ \ Error = \frac{1}{n}\sum_{j=1}^{n}\frac{q''_{c,cal,j} - q''_{c,exp,j}}{q''_{c,exp,j}}$$

$$RMS\ \ Error = \sqrt{\frac{1}{n}\sum_{j=1}^{n}\left(\frac{q''_{c,cal,j} - q''_{c,exp,j}}{q''_{c,exp,j}}\right)^2} \tag{22}$$

$$Standard\ \ Deviation = \sqrt{\frac{1}{n-1}\sum_{j=1}^{n}\left(\frac{q''_{c,cal,j}}{q''_{c,exp,j}} - \frac{1}{n}\sum_{j=1}^{n}\frac{q''_{c,cal,j}}{q''_{c,exp,j}}\right)^2}$$

Shown as figures, case 4 exhibits the best results. Case 4 used the Sugawara correlation for entrainment and deposition of liquid droplets and the Chun correlation for the criterion of the dryout point.

Although the Ezzidi correlation is an improved form of the Sugawara correlation, as mentioned above, the result of applying the Sugawara correlation was better

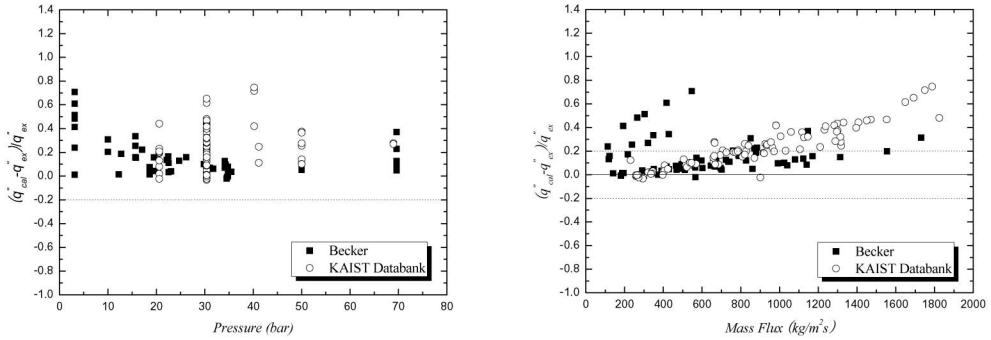

Relative Error vs. Pressure Relative Error vs. Mass Flux

Fig. 3. **Wurtz** Correlation for Entrainment/Deposition, **without** Critical Thickness for Dryout (Case 1)

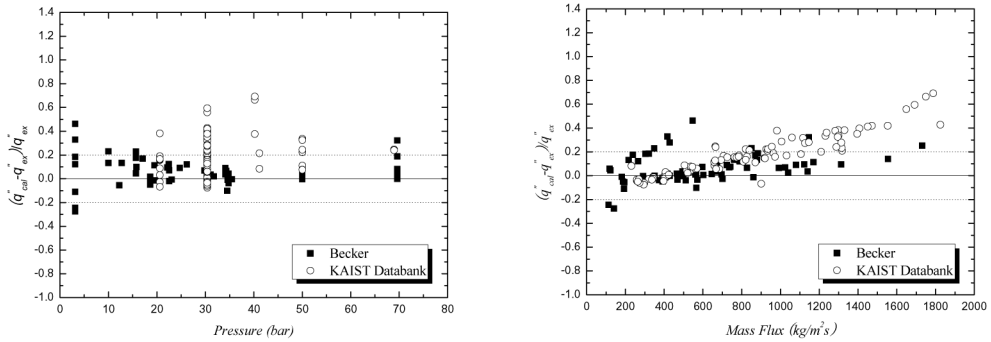

Relative Error vs. Pressure Relative Error vs. Mass Flux

Fig. 4. **Wurtz** Correlation for Entrainment/Deposition, **with** Critical Thickness for Dryout (Case 2)

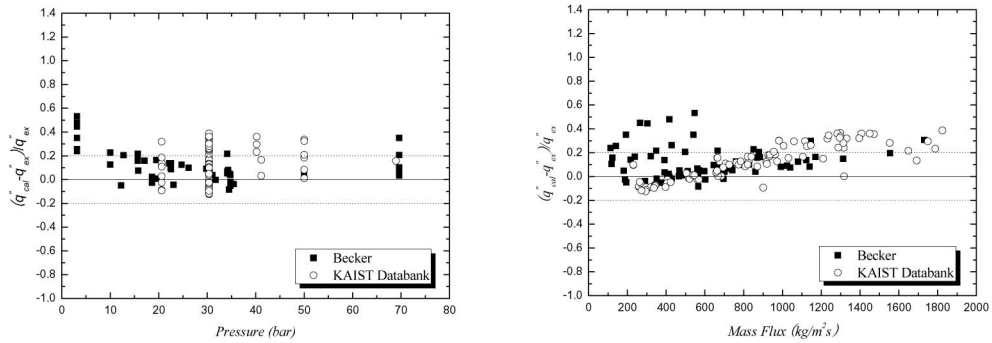

Relative Error vs. Pressure Relative Error vs. Mass Flux

Fig. 5. **Sugawara** Correlation for Entrainment/Deposition, **without** Critical Thickness for Dryout (Case 3)

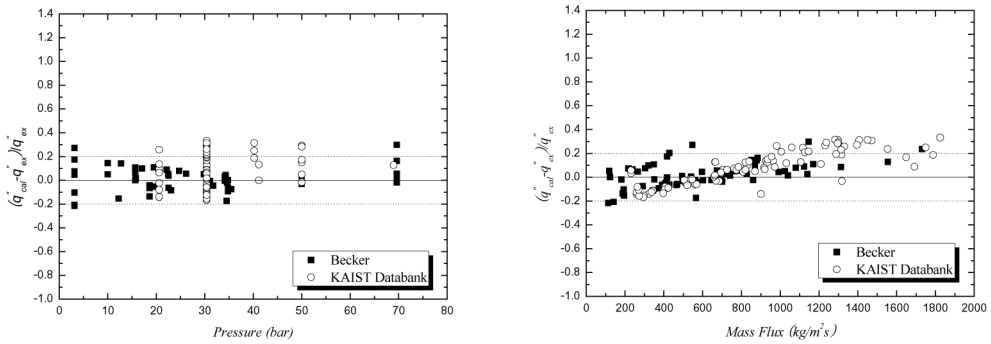

Relative Error vs. Pressure Relative Error vs. Mass Flux

Fig. 6. **Sugawara** Correlation for Entrainment/Deposition, **with** Critical Thickness for Dryout (Case 4)

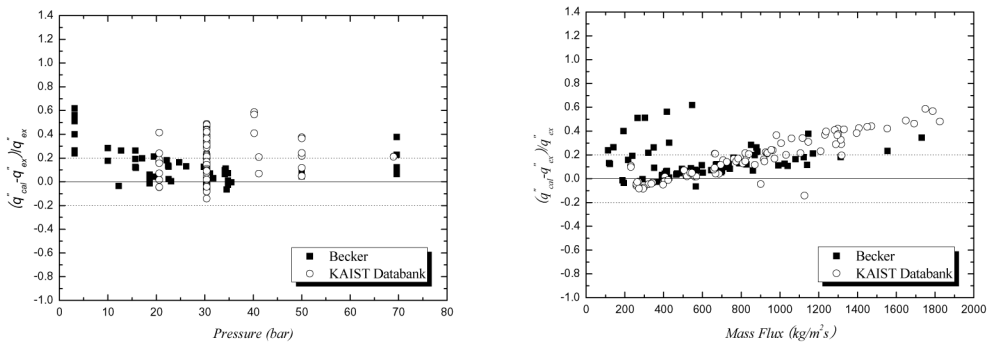

Relative Error vs. Pressure Relative Error vs. Mass Flux

Fig. 7. **Ezzidi** Correlation for Entrainment/Deposition, **without** Critical Thickness for Dryout (Case 5)

than the result of applying the Ezzidi correlation. This can be explained by the following points. The first point is that the improvement of the Ezzidi correlation is limited to the COBRA-TF, because the improvements were performed on the COBRA-TF code, making them COBRA-TF-code dependent. It cannot, therefore, be generalized that the Ezzidi correlation is better than the Sugawara correlation. The second point is that the accuracy of dryout does not depend on the accuracy of only one model; the combination of each model is more important. We can say that the combination of the Sugawara correlation with the drift-flux model is better than the combinations employing the Ezzidi correlation.

The cases with the critical thickness concept generally had good results that diminished large errors in the high mass flux regions. This resulted from the effect

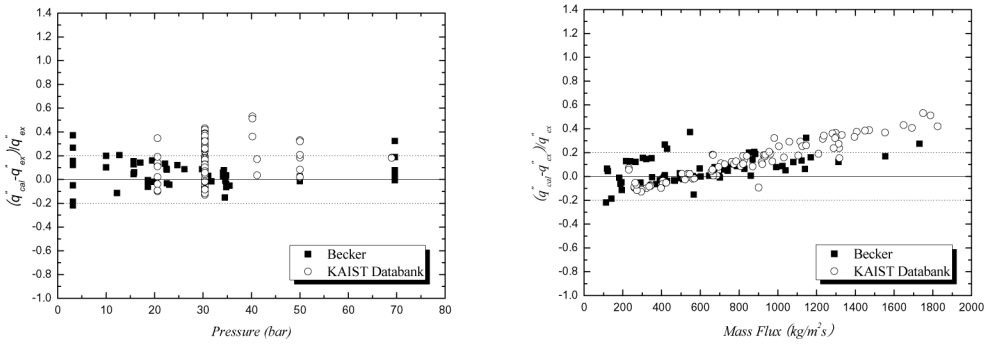

Relative Error vs. Pressure Relative Error vs. Mass Flux

Fig. 8. **Ezzidi** Correlation for Entrainment/Deposition, **with** Critical Thickness for Dryout (Case 6)

Table 4. Statistics of Each Case

Case	Mean Error	RMS Error	Standard Deviation
Case 1	0.18729	0.24989	0.16596
Case 2	0.12666	0.20458	0.16116
Case 3	0.11797	0.18241	0.13957
Case 4	*0.04997*	*0.13933*	*0.13047*
Case 5	0.16100	0.22738	0.16107
Case 6	0.09872	0.17954	0.15044

of the heat flux and liquid mass flux terms in the correlation.

Based on our results, we finally selected the optimized annular flow dryout model as shown in Table 5. This model has a prediction ability with a mean error of 0.04997, RMS error of 0.13933, and a standard deviation of 0.13047.

The model proposed in this study was compared with MARS code to assess its prediction ability. As shown in the Fig. 9 and Table 6, the results of this model were better than those of the MARS code. We can therefore say that this model is not only simpler than MARS code, but also better than MARS code for performing dryout calculations.

5. CONCLUSION

Development of experimental approaches to the measurement of annular flow dryout demands parallel development of numerical models of annular flow dryout. The key requirements for a numerical dryout model are

Table 5. Optimized Annular Flow Dryout Model

Flow Regime	Applied Models
Sub-cooled Single Phase	- Heat Balance of Single Phase ***(Eq. 1)***
Bubbly and Slug	- ***Zuber*** **drift velocity model** to determine the velocity and fraction of each phase ***(Eq. 5)***
Annular	- ***Sugawara*** **correlation** for entrainment/deposition ***(Eq. 18 and 19)*** - ***Ishii*** **drift velocity model** to determine the velocity and fraction of each phase ***(Eq. 12)***
Dryout	- Criterion of dryout ***with*** **Chun critical thickness correlation** ***(Eq. 21)***

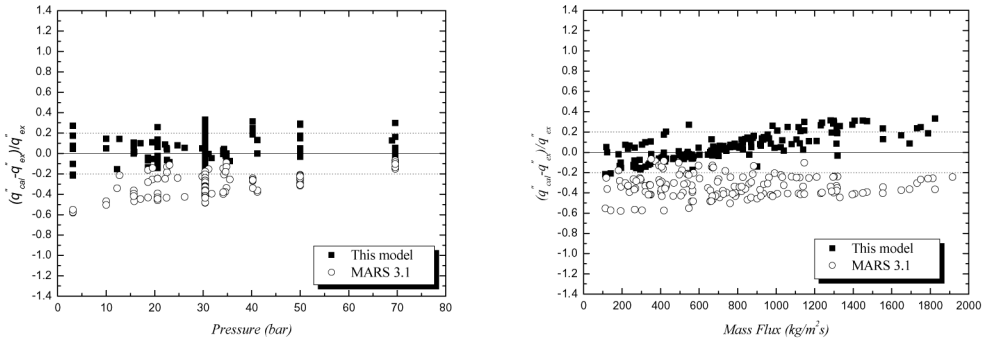

Relative Error vs. Pressure Relative Error vs. Mass Flux

Fig. 9. Comparison of Proposed Model with MARS Code

Table 6. Statistical Comparison of Proposed Model with MARS Code

Code	Mean Error	RMS Error	Standard Deviation
This model	0.04997	0.35209	0.13047
MARS code	- 0.3344	0.13933	0.11046

the accurate determination of the velocities and fraction of each phase, and a combination of models that apply to these parameters. To determine the velocities and fractions of each phase, the drift-flux model was used in this study. Additionally, three candidates for entrainment and deposition correlations, and two criteria of the dryout point were selected. Entrainment, deposition, and criterion of dryout are important parameters which strongly affect the accuracy of dryout calculations. Through comparison with experimental CHF data, the optimized combination for an annular flow dryout model was determined to be the drift-flux model with the Sugawara entrainment/deposition model and critical thickness concept as the criterion of the dryout point. This model showed reasonable results with a mean error of 0.04997, RMS error of 0.13933, and a standard deviation of 0.13047. These results were better than the results of MARS code.

NOMENCLATURE

q'' : heat flux
D : diameter of tube
G : mass flux
C_{pl} : specific heat at constant pressure of single phase liquid
T : temperature of fluid
z : axial location
u : velocity
V_{gj} : drift velocity
j : volumetric flux
x : quality
$\dot{m}$: mass flow rate
h_{fg} : latent heat
P_W : wetted perimeter
f_i : interfacial friction factor
k_s : equivalent sand roughness
C_D : mean concentration of liquid droplet in the core
Δh_{eq} : hydraulic equivalent sand roughness
Re : Reynolds number
Sc : Schmidt number

Greek Symbols

ρ : density
α : void fraction
δ : liquid film thickness
τ_i : interfacial shear stress

Subscript

sat : saturated condition
l : single phase liquid
in : inlet
g : vapor at saturated condition
f : liquid at saturated condition
e : liquid droplet
SA : transition from slug to annular flow regime
evap : evaporation
ent : entrainment
dep : deposition
c : critical heat flux (dryout)
critical : critical thickness

REFERENCES

[1] Collier, J. G., *Convective Boiling and Condensation*, 2nd Edition, McGRAW-HILL International Book Company (1980).
[2] Zuber, N., et al., "Steady State and Transient Void Fraction in Two-Phase Flow Systems," GEAP 5417 (1967).
[3] INEEL. "RELAP5/MOD3 Code Manual Volume IV: Models and Correlations," NUREG/CR-5535, USNRC (1998)
[4] Ishii, M., et al., "Constitutive Equation for Vapor Drift Velocity in Two-Phase Annular Flow," *AIChE Journal*, Vol. 22, pp. 283-289 (1976)
[5] Wurtz, J., et al., "An Experimental and Theoretical Investigation of Annular Steam-Water Flow in Tubes and Annuli at 30 to 90 bar," No.372, Riso report (1978).
[6] Sugawara, S., "Droplet Deposition and Entrainment Modeling Based on the Three-Fluid Model," *Nuclear Engineering and Design*, Vol. 122, pp. 67-84 (1990)
[7] Ezzidi, A., et al., "Improvement of COBRA-TF Code Models for Liquid Entrainments in Film-Mist Flow," JAERI-M 93-133 (1993)
[8] Chun, J. H., et al.. "Development of the Critical Film Thickness Correlation for and Advanced Annular Film Mechanistic Dryout Model Applicable to MARS Code," *Nuclear Engineering and Design*, Vol. 223, pp. 315-328 (2003)
[9] Becker, K. M., et al., "Burnout Data for Flow of Boiling Water in Vertical Round Ducts, Annuli and Rod Clusters," AE-177 (1965).
[10] Chang, S. H. and Baek, W. P., *The KAIST CHF Data Bank (Rev. 3)*, KAIST-NUSCOL-9601 (1996).